Cancer Letters 450 (2019) 63–75

Contents lists available at ScienceDirect

Cancer Letters

journal homepage: www.elsevier.com/locate/canlet

Original Articles

Long non-coding RNA FGF13-AS1 inhibits glycolysis and stemness properties of breast cancer cells through FGF13-AS1/IGF2BPs/Myc feedback loop

Fei Ma[a], Xu Liu[a], Shibo Zhou[c], Wenjie Li[a], Chunxiao Liu[a], Michelle Chadwick[d], Cheng Qian[a,b,*]

[a] Department of Breast Surgery, Harbin Medical University Cancer Hospital, Harbin, China
[b] Translational Medicine Research and Cooperation Center of Northern China, Heilongjiang Academy of Medical Sciences, Harbin, China
[c] Department of Pharmacy, The Fourth Affiliated Hospital of Harbin Medical University, Harbin, China
[d] Cancer Institute of New Jersey, Rutgers University, New Brunswick, United States

ARTICLE INFO

Keywords:
Lnc FGF13-AS1
Metabolism
Stemness
c-Myc

ABSTRACT

LncRNAs have been proven to play crucial roles in various processes of breast cancer. LncRNA FGF13-AS1 has been identified as one of the 25 downregulated lncRNAs in breast cancer through analyzing data from two cohorts and TCGA by another group of our lab. In this study, we report that FGF13-AS1 expression is decreased in breast cancer tissue compared with corresponding normal tissue, and the downregulation of FGF13-AS1 is associated with poor prognosis. Functional studies show that FGF13-AS1 inhibits breast cancer cells proliferation, migration, and invasion by impairing glycolysis and stemness properties. Mechanistically, FGF13-AS1 reduces the half-life of c-Myc (Myc) mRNA by binding RNA-binding proteins, insulin-like growth factor 2 mRNA binding proteins (IGF2BPs) and disrupting the interaction between IGF2BPs and Myc mRNA. Furthermore, Myc transcriptionally inhibits FGF13-AS1, forming a feedback loop in this signaling pathway. These results reveal for the first time that FGF13-AS1 functions as a tumor suppressor by inhibiting glycolysis and stemness properties of breast cancer cells, and the FGF13-AS1/IGF2BPs/Myc feedback loop could be a novel therapeutic target for breast cancer patients.

1. Introduction

As a highly heterogeneous malignancy, breast cancer is the most prevalent cancer in women, and its incidence is still increasing rapidly [1]. Although great efforts have been made to reveal the genetic and epigenetic changes in breast cancer, the precise mechanism that cause tumor progression remains to be further studied [2,3]. Given that breast cancer relapse and metastasis are frequently associated with cell glycolysis and stemness properties [4,5], elucidating the fundamental mechanism that regulates tumor cell glycolytic metabolism and stem-like properties are of great importance, and may open up new avenues for potential therapeutic exploitation.

Recent studies have demonstrated that Myc (c-Myc), a well-established oncogenic transcription factor, controls many processes of cancer cells, including cell growth, glycolytic metabolism, proliferation, apoptosis and cell stemness [6–9]. For example, Myc has been shown to activate several glucose transporters and glycolytic enzymes, such as lactate dehydrogenase A (LDHA) and pyruvate dehydrogenase kinase 1 (PDK1) [10,11]. Moreover, Myc is also reported to activate breast cancer stemness and support the self-renewal features of breast cancer cells [12]. Thus, treatments targeting Myc for breast cancer therapy attract much attention. Strategies interacting with Myc activation and downstream targets are being developed. However, due to its special structure and function as a transcription factor, direct interaction with Myc fails to show good therapeutic effects. Therefore, inhibiting Myc on post-transcriptional or translational level may represent an effective approach to treat Myc-driven cancers.

Protein-coding genes account for only 2% of the human genome, whereas the majority of transcripts are composed of the non-protein-coding RNAs [13]. Long non-coding RNAs (lncRNAs), which belong to non-protein-coding RNAs, are greater than 200 nt in length and are characterized by the complexity and diversity of their action mechanisms and sequences [14]. Despite being newly identified, they have been found to play crucial roles in the regulation of various cellular processes and disease progressions, including stem-like state, glucose metabolism and tumor metastasis [15–17]. To exercise their functions,

* Corresponding author. Department of Breast Surgery, Harbin Medical University Cancer Hospital, Harbin, China.
E-mail address: qiancheng@ems.hrbmu.edu.cn (C. Qian).

https://doi.org/10.1016/j.canlet.2019.02.008
Received 29 June 2018; Received in revised form 24 January 2019; Accepted 10 February 2019

lncRNAs can serve as decoys, scaffolds or guides. For example, lncRNAs can associate with regulatory RNAs or proteins, and prevent them from binding to specific target mRNAs or chromatin loci or inhibit the activity of enzymes [18–21]. Notably, inhibitors of the antisense transcript class of lncRNAs can be designed, which highlights the significance of developing new target lncRNAs for cancer treatment [22]. Recently, another group in our lab identified lncRNA FGF13-AS1 (FGF13-AS1) as one of the 25 downregulated lncRNAs in breast cancer by analyzing data from two cohorts and TCGA [23]. However, no studies have explored the role or functional mechanism of FGF13-AS1 in breast cancer.

In this study, we show that FGF13-AS1 is downregulated in breast cancer and that low expression of FGF13-AS1 is associated with poor prognosis. Functional studies show that FGF13-AS1 inhibits breast cancer cell proliferation, migration and invasion by impairing glycolysis and stemness properties. Mechanistically, FGF13-AS1 functions as a negative regulator of Myc mRNA by binding RNA-binding proteins, insulin-like growth factor 2 mRNA binding proteins (IGF2BPs) and disrupting the interaction between IGF2BPs and Myc mRNA. Furthermore, Myc is found to transcriptionally inhibit FGF13-AS1 which exerts a feedback loop on this axis.

2. Materials and methods

2.1. Cell lines and human breast cancer specimens

All breast cancer cell lines (MCF-10A, MCF-7, T47D, MDA-MB-453, MDA-MB-468, MDA-MB-231) and the human 293T cell line were obtained from the Chinese Type Culture Collection, Chinese Academy of Science. 293T, MCF-10A, MCF-7, T47D and MDA-MB-453 cells were maintained in DMEM supplemented with 10% fetal bovine serum. MDA-MB-468 and MDA-MB-231 cells were cultured in Leibovitz's L-15 Medium containing 10% FBS. All the cells were cultured in a humidified atmosphere containing 5% CO2 and at 37 ˚C.

Fresh breast cancer tissues and paired adjacent non-tumor breast tissues were obtained from 60 patients who underwent surgery in the Department of General Surgery of the Second Affiliated Hospital of Harbin Medical University between Jan 2012 and Jan 2014. None of the patients received any anticancer treatments including radiotherapy or chemotherapy before the surgery. The correlated clinical information of the patients was collected and analyzed. All the patients provided written consent according to the ethical standards of Declaration of Helsinki. The study was approved by the ethics and scientific committee of Harbin Medical University. The stage of breast cancer was determined according to the TNM classification proposed by the AJCC cancer staging manual. The samples were immediately frozen at − 80 ˚C after surgical resection.

2.2. Real-time quantitative PCR

Total RNA was extracted with Trizol reagent (Invitrogen, USA). cDNA was synthesized under the standard conditions. Real-time PCR was performed by using the SYBR Green kit (Thermo Fisher, USA) following the manufacturer's instructions. The expression of FGF13-AS1 and Myc mRNA level were normalized to 18S tRNA for each sample. The primers for real-time quantitative PCR detection are listed as follows: FGF13-AS1, 5′-TCTCCAACAGGAAACTATGCCA-3′ (forward) and 5′-TCCTGGAGATGCCTCTTGAGA-3′ (reverse); Myc, 5′-TGAGGAGACA CCGCCCAC-3′ (forward) and 5-CAACATCGATTTCTTCCTCATCTTC-3′ (reverse); 18S rRNA, 5′-GTAACCCGTTGAACCCCATT-3′ (forward) and 5′-CCATCCAATCGGTAGTAGCG-3′ (reverse). The real-time quantitative PCR reactions were repeated three times. Relative RNA expression was calculated by deltaCt method. The samples were divided into high and low FGF13-AS1 expression groups according to the qRT-PCR detection. Samples with FGF13-AS1 expression greater than the median value were put into high FGF13-AS1 expression group; samples with FGF13-AS1 expression less than the median value were put into the low FGF13-AS1 expression group.

2.3. Lentiviral infection and transient transfection

To construct stably FGF13-AS1-overexpressed cell lines, indicated breast cancer cells were infected with Lv-FGF13-AS1 and Lv-con virus (LAND, Guangzhou, China). Lv-sh-FGF13-AS1 and Lv-sh-control were purchased from GeneChem (Shanghai, China). Infection was performed in the presence of 8 μg/ml polybrene for 24 h followed by puromycin selection. The expression of FGF13-AS1 was determined by qRT-PCR assays. We designed three shRNAs targeted FGF13-AS1, and the sequences of shRNA used for constructs are listed below: FGF13-AS1-shRNA#1: 5′-AGUUUGUUCUCCUUCUACACU-3′ (sense), 5′-UGUAGA AGGAGAACAAACUGG-3′ (antisense); FGF13-AS1-shRNA#2: 5′-CAAC UGGAUAGAAAUACAAAU-3’ (sense), 5′-UUGUAUUUCUAUCCAGUU GUU-3′ (antisense). FGF13-AS1-shRNA#3: 5′-GGACUGAUGAUGAGCU CAA-3′ (sense), 5′-UUGAGCUCAUCAUCAGUCC-3′ (antisense). Small interfering RNA (siRNA), si-IGF2BPs, si-control were purchased from Santa Cruz Biotechnology (Santa Cruz, CA, USA) and GenePharma (Shanghai, China). The siRNA specifically targeting Myc was synthesized from GenePharma (Shanghai, China). Transient transfections were performed using Lipofectamine 2000 (Invitrogen) following the manufacturer's instructions. After 48 h, the transfected cells were harvested.

2.4. 3-(4,5-Dimethylthiazol-2-yl)-2,5-diphenyltetrazolium bromide (MTT) assay

2×10^3 cells were seeded in each well of a 96-well plate. At each time point, the indicated cells were stained with 100 μl MTT solution (Abcam) at 37 ˚C for 3 h. After incubation, 150 μl solvent was added into each well and the plate was wrapped in foil and shaken for 15 min. Then the absorbance was read at 570 nm. All experiments were performed three times.

2.5. Colony formation assay

Indicated breast cancer cells were seeded in 12-well plates at the density of 250 cells each well and cultured in medium for 14 days. The cells were washed with PBS and fixed in methanol for 20 min. The cells were then stained with crystal violet for 15 min, after which they were photographed by digital camera.

2.6. Migration and invasion assay

The migration and invasion of indicated cells were detected using 24-well transwell plates (Corning Costar, Tewksbury, MA, USA). For the migration assays, 10^5 cells were seeded into the upper chamber of each insert with 200 μl serum-free medium and 600 μl medium with 10% FBS was added into the lower chambers. After incubating at 37 ˚C for 24 h, the cells on the top side of the membrane were removed by cotton swabs and the cells invaded to the underside of the membrane were fixed with 4% paraformaldehyde and stained with crystal violet. Then the cells were counted and imaged under a microscope. For the invasion assays, the upper chambers of the insert were coated with Matrigel (BD Bioscience, USA) and dried at 37 ˚C for 3 h. Then the cells were plated on the top of the Matrigel. All the experiments were performed triplicate.

2.7. 3D morphogenesis matrigel culture

5×10^3 indicated cells were resuspended in 300 μl Matrigel matrix solution (Corning Life Science) on ice and were seeded in each well of a 24-well plate coated with Corning Matrigel Matrix (Corning Life Science). The plate was then incubated at 37 ˚C for 30 min to solidify

the gel, and 500 µl complete medium of indicated cells was gently added on top of the Matrigel. The medium was changed every other day. After 2 weeks, the 3D-cultured spheroids were counted and imaged under a microscope.

2.8. $CD44^+CD24^-$ phenotype proportions

Indicated breast cancer cells were dissociated and resuspended as single cells in PBS with 5% FBS. Then the cells were incubated with FITC anti-CD44 and PE anti-CD24 for 15 min at 4 °C in a dark room. Analysis was conducted using a FACS Aria II cell sorter (BD, Bioscience, USA).

2.9. Immunofluorescence staining and fluorescence in situ hybridization (FISH)

The 3D-cultured spheroids in Matrigel were fixed with 4% formaldehyde for 10 min and permeabilized with 0.5% Triton X-100 overnight. After blocking with 5% BSA, the indicated spheroids were incubated with primary antibodies: anti-Oct4, anti-SOX2 (Cell Signaling Technology). They were then incubated with corresponding secondary antibodies (Cell Signaling Technology) and DAPI (Thermo Fisher Scientific). Images were taken using confocal microscopy. To detect FGF13-AS1 expression in breast cancer cells, lncRNA FISH Probe Mix and Fluorescence In Situ Hybridization Kit (RIBO Bio, China) were used for the FISH detection. Cells were washed in PBS and fixed in 4% formaldehyde for 10 min at room temperature. Then cells were permeabilized with 0.5% Triton X-100 at 4 °C for 5 min. Next the hybridization was performed following the manufacture's protocol. FGF13-AS1 was measured under confocal microscopy. To detect expression of Myc, cells were fixed again with 4% formaldehyde and subjected to standard immunofluorescence staining. The anti-Myc and secondary antibodies were purchased from Cell Signaling Technology. DAPI (Thermo Fisher Scientific) was used to stain nuclei.

2.10. Glycolysis stress test

Briefly, indicated cells were cultured in stress test medium without glucose. After the addition of saturating amounts of glucose, the extracellular acidification rate (ECAR) was measured by the Seahorse XF96 Analyzer Glycolysis. The rapid increase in ECAR is regarded as the glycolysis rate under basal conditions. Next, with the addition of oligomycin, the oxidative phosphorylation was shut down and the maximum ECAR rate was measured again. The maximum ECAR rate revealed the glycolytic capacity of the cells. Thirdly, the glucose analog, 2-deoxyglucose (2-DG), was added into the system. This led to a decrease of ECAR rate which indicated that the ECAR production was from the glycolysis. The gap between the glycolytic capacity and glycolysis rate represented the glycolytic reserve, which indicated the capability of the cells to respond to an energetic demand.

2.11. Glucose consumption and lactate production

Glucose consumption and lactate production were measured as previously described [5].

2.12. Western blot

Indicated cells were lysed in RIPA lysis buffer with protease inhibitor. Cell lysates were extracted and separated by 10% SDS gel electrophoresis. Then the protein was transferred to a PVDF membrane (Millipore, USA). Next the membrane was blocked with 5% non-fat dry milk and followed by incubated with primary antibodies: anti-Myc, anti-HIF-1α, anti-IGF2BP1 and anti-GAPDH. All the antibodies were purchased from Cell Signaling Technology. Secondary antibodies were then incubated with the membranes for 1.5 h. ECL detection reagents (Thermo Fisher Scientific) were used to detect the signals. The densities of specific proteins were normalized to the density of GAPDH.

2.13. Nuclear and cytoplasmic RNA isolation

Indicated cells were washed with cold PBS three times. Then the PARIS Kit (Life Technologies, CA, USA) was used to isolate the cytoplasmic fraction following the manufacturer's protocol. Briefly, cells were lysed with cell fractionation buffer and incubated on ice for 10 min. By centrifuging at 500 g for 5 min, the supernatant was collected as cytoplasmic fraction and the remaining nuclear pellets were lysed by cell disruption buffer as nuclear fraction. Next the RNA of the cytoplasmic and nuclear fraction was extracted according to the protocol. The nuclear and cytoplasmic RNA was further analyzed by qRT-PCR.

2.14. Luciferase reporter assay

Luciferase reporter assays were performed with the Dual Luciferase Assay System (Promega, USA) according to the manufacturer's protocol. Briefly, 293T cells were co-transfected with various amount of Myc overexpression plasmid, 0.2 µg wild-type FGF13-AS1 promoter-luciferase reporter plasmid or 0.2 µg mutant FGF13-AS1 promoter-luciferase reporter plasmid and 0.02 µg pRL-TK plasmid (Promega, USA). The FuGENE HD reagent was used for DNA transfection. Cells were lysed by 1× passive lysis buffer 48 h after transfection. 20 µl of each lysate were transferred to a 96-well plate and detected with a luminometer using the Dual Luciferase Assay System (Promega). For each experiment, the firefly luciferase activity was normalized to the activity of the Renilla luciferase used as an internal control.

2.15. Chromatin-immunoprecipitation (ChIP)

For ChIP assays, the EZ ChIP Kit (Millipore) was used following the manufacturer's instruction. Briefly, indicated breast cancer cells for each reaction were collected and crosslinked with 1% formaldehyde at room temperature. Then glycine was added to stop the reaction and the cells were incubated with lysis buffer containing protease inhibitor on ice for 30 min. Cells were then sheared by sonication on ice and centrifuged. Protein A agarose (Roche, USA) was added into the supernatant and the supernatant was incubated with anti-Myc or IgG antibody (Cell Signaling Technology) overnight. After the DNA purification, PCR was performed to amplify the target sequences from the immunoprecipitated DNA samples and the input. The primers used for detecting the FGF13-AS1 promoter were listed below: 5′-TCCTCATCT TTGGTGCCATCA-3' (forward) and 5′-TGTTTTCTTTCTTCCAGACACCT TAA-3' (reverse). PCR products were run on 3% agarose gels to present FGF13-AS1 promoter fragments.

2.16. RNA pull-down assay

All experiments were performed in RNase-free conditions. FGF13-AS1 and its antisense RNA were transcribed in vitro and biotin-labeled using Biotin RNA Labeling Mix (Roche). Next the biotin-labeled RNA oligomers (100 pmol) were incubated with protein lysates (2 mg) from MDA-MB-231 cells. One hour after the incubation, streptavidin agarose beads (Invitrogen) were added to the reaction mix to isolate the RNA-protein complex. After three washes at room temperature, the retrieved protein was subjected to normal western blot analysis.

2.17. RNA immunoprecipitation (RIP)

RIP assays were performed using the Magna RIP RNA-binding protein immunoprecipitation kit (Millipore, USA) following the manufacturer's instructions. Briefly, 2×10^7 cells were lysed in RIP Lysis buffer and transferred to nuclease-free tubes on ice. Then the resuspended beads were incubated with indicated antibodies for 30 min at room temperature. The RIP lysate was then added to the beads-antibody complex in RIP immunoprecipitation buffer. After extensive washing, the bead-bound immunoprecipitate was eluted with elution buffer at 55 °C for

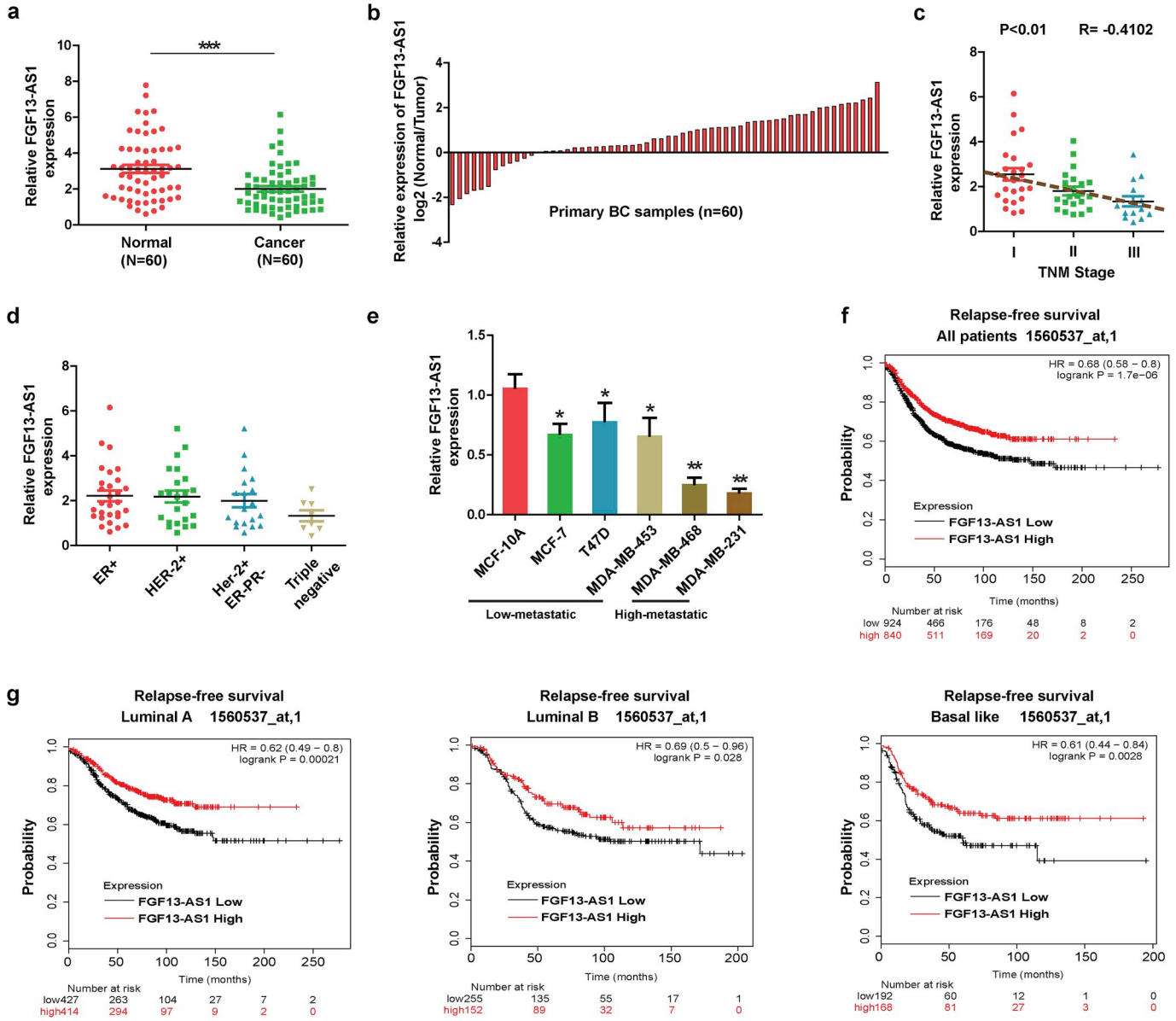

Fig. 1. The expression level of FGF13-AS1 in breast cancer and the association between FGF13-AS1 expression and prognosis. (**a**) and (**b**) Real-time quantitative PCR was used to detect the expression level of FGF13-AS1 in breast cancer tissues and corresponding normal tissues in 60 patients. (**c**) Relative expression of FGF13-AS1 was measured in breast cancer tumors from patients of different stages by qRT-PCR. (**d**) and (**e**) The expression of FGF13-AS1 in different breast cancer cell lines and different receptor types of breast cancer tissue. (**f**) Kaplan-Meier Plotter was used to analyze the relationship between FGF13-AS1 expression and relapse-free survival in a group of 1764 patients. (**g**) The relationship between FGF13-AS1 expression and relapse-free survival was detected in different breast cancer subtypes (luminal A, luminal B and basal-like). *P < 0.05, **P < 0.01, ***P < 0.001, # represents no statistical significance.

30 min. Phenol/chloroform/isoamyl alcohol was used to isolate protein associated RNAs from the eluted immunoprecipitate. Purified RNAs were then subjected to qRT-PCR or reverse transcription PCR. The primers specific to FGF13-AS1 immunoprecipitate sequence are listed below: 5′-TCACTTGCCAGTTTGTTCTCCT-3' (forward) and 5′-ACTTGGCTACCT CATCTCGT-3' (reverse). The primers specific to Myc immunoprecipitate sequence are listed below: 5′-GCATACATCCTGTCCGTCCA-3' (forward) and 5′-GTCGTTTCCGCAACAAGTCC-3' (reverse).

2.18. In situ hybridization (ISH)

The expression of FGF13-AS1 in tumor tissues were detected using the Biochain In Situ Hybridization Kit (Biochain) following the manufacturer's instructions. Briefly, tissues were deparaffinized and fixed in 4% paraformaldehyde in DEPC-PBS and then digested with 0.1% Triton-X and 2X standard saline citrate. Prehybridized with prehybridization solution, the tissues were then incubated with hybridization buffer and digoxigenin labeled probe (EXIQON). The tissues were incubated with the AP-conjugated anti-digoxingenin antibody. Further, the slides were washed and visualized with NBT/BCIP (Pierce). The images were taken and analyzed under a microscope.

2.19. Immunohistochemistry

The paraffin-embedded tumor samples from patients or mice were deparaffinized in xylene, rehydrated and blocked in 10% goat serum. Then the samples were incubated with the Myc primary antibody (Abcam) overnight and subsequently followed by HRP secondary antibody (Abcam). After staining, the slides were visualized and imaged under a microscope.

2.20. Animal models

All the procedures involved in animal experiments were performed in accordance with the Guide for the Administration of Affairs Concerning Experimental Animals, the national guideline for animal experiments. Female NOD/SCID mice (Vital Rivers, China) were housed in a specific pathogen free barrier facility with an 12 h light/dark cycle. For the tumorigenesis assays, MDA-MB-231-Luc breast cancer cells (5×10^5) transfected with FGF13-AS1 or control were injected orthotopically into the fat pad of 6-week-old female mice. Tumor growth was monitored every week and the tumors were collected after 4 weeks. For the tumor metastasis model, MDA-MB-231-Luc breast cancer cells (5×10^5) transfected with FGF13-AS1 or control were injected into the tail vein of mice. By the end of 6 weeks, after intraperitoneal injection of D-luciferin, all mice were imaged by the Xenogen IVIS Spectrum Imaging System (Caliper Life Sciences, USA) before being sacrificed. Primary tumor volume and the number of lung metastatic nodes were measured. For each tissue, HE or IHC staining was performed for histological detection. All the animal assays were approved by the Animal Experimental Ethics Committee of Harbin Medical University.

2.21. Statistical analysis

Quantitative data in this study were presented as mean ± standard deviation from at least three replicates were analyzed by the two-tailed unpaired Student's t-test to compare the difference between groups. Statistical analysis was performed by Graphpad Prism 7. A $P < 0.05$ was regarded to be statistically significant.

3. Results

3.1. The expression of FGF13-AS1 is decreased in breast cancer which is associated with poor prognosis

By genome-wide in silico analysis, FGF13-AS1 was identified as one of the 25 downregulated lncRNAs in breast cancer tissues by another group in our lab [23]. However, no biological experiments were performed to confirm the expression of FGF13-AS1 in breast tissues. We set out to examine the expression level of FGF13-AS1 in normal breast and breast cancer tissues in a group of 60 patients. As shown in Fig. 1a, the expression level of FGF13-AS1 was significantly lower in the breast cancer group compared with the corresponding normal breast tissue group. Compared with counterparts, the level of FGF13-AS1 was decreased in 48 of the 60 (80%) breast cancer tissues (Fig. 1b). To explore the clinical significance of FGF13-AS1 down-regulation in breast cancer, we assessed the relevance between FGF13-AS1 expression and clinicopathologic futures of the patients. We found that FGF13-AS1 expression was negatively correlated with lymph node metastasis and tumor stage of breast cancer (Fig. 1c and Table 1). Consistent with these results, we observed that the expression of FGF13-AS1 was much lower in highly metastatic BC cell lines than that in low-metastatic BC cell lines (Fig. 1e). However, no difference of FGF13-AS1 expression was found between any two receptor types of breast cancer (Fig. 1d). Based on this expression pattern, we chose two pairs of cell lines (MCF-7/MDA-MB-231 and T47D/MDA-MB-468) for following functional studies. A Kaplan-Meier Plotter (KM Plotter; kmplot.com) was used to analyze microarray data from 1764 patients to correlate FGF13-AS1 expression with patient survival. The analysis results indicated that patients with low expression of FGF13-AS1 tend to have worse relapse-free survival (Fig. 1f). This was also the case when we divided the patients into luminal A, luminal B and basal-like subtypes (Fig. 1g). Taken together, these data suggest that FGF13-AS1 expression is decreased in breast cancer and the downregulation of FGF13-AS1 is associated with poor prognosis.

Table 1
Relationship between FGF13-AS1 expression and clinicopathologic features of BC patients (n = 60).

variable	Relative FGF13-AS1 expression		P-value
	Low (n = 30)	High (n = 30)	
Age			NS
< 50	18	14	
> 50	12	16	
Histological differentiation			NS
Well	10	14	
Moderate	13	12	
Poor	7	4	
Tumor size			NS
< 2 cm	10	18	
2–5 cm	12	8	
> 5 cm	8	4	
Lymph node metastasis			P < 0.05
Yes	19	10	
No	11	20	
Tumor stage			P < 0.05
I	8	17	
II	12	9	
III	10	4	
Molecular subtype			NS
Luminal like	15	18	
Her-2	10	9	
Triple negative	5	3	

Note: BC patients were divided into FGF13-AS1 high group and low group according to the analysis of qRT-PCR detection. NS, not significant between different groups. Differences among variables were evaluated by χ^2 or Fisher's exact χ^2 -test.

3.2. FGF13-AS1 inhibits breast cancer cells proliferation, invasion and metastasis both in vitro and in vivo

Given the relationship between FGF13-AS1 expression and breast cancer prognosis, we further explored the biology function of FGF13-AS1 in breast cancer. We infected breast cancer cells with lentiviral constructs expressing FGF13-AS1 and sh-FGF13-AS1. Real-time PCR was used to confirm the remarkable expression (Supplementary Fig. 1 and 2a). As indicated in Fig. 2b, FGF13-AS1 overexpression markedly suppressed the proliferation of MDA-MB-231 cells. Conversely, knockdown of FGF13-AS1 by siRNA promoted the growth of MCF-7 cells (Fig. 2a and Supplementary Fig. 2b). Colony formation assays also showed similar results in indicated cells (Fig. 2c and Supplementary Fig. 2c). Next, we tested the effect of FGF13-AS1 on the migratory and invasive abilities of breast cancer cells. Matrigel-coated and non-coated transwell assays indicated that suppression of FGF13-AS1 dramatically increased the invasion and migration of MCF-7 cells, whereas FGF13-AS1 overexpression in MDA-MB-231 cells decreased the invasive and migratory abilities of cancer cells (Fig. 2d and Supplementary Fig. 2d). To verify the effect of FGF13-AS1 in vivo, MDA-MB-231 cells were orthotopically injected into the mammary fat pads of SCID mice. We noted that compared with the control groups, cells transfected with FGF13-AS1 showed decreased growth ability (Fig. 2e and Supplementary Fig. 2e). Meanwhile, the expression of FGF13-AS1 in xenograft tumors was also confirmed by qRT-PCR and ISH (Supplementary Fig. 3e). A lung metastasis mouse model was also established through tail vein injection to further confirm the role of FGF13-AS1 in breast cancer metastasis in vivo. Results revealed that mice injected with FGF13-AS1-overexpressing cells had less lung metastatic nodes than those injected with control cells. Conversely, knockdown of FGF13-AS1 in MCF-7 cells markedly increased the xenograft tumor size and number of lung metastatic nodes in this mouse model (Fig. 2f and Supplementary Fig. 2f). This effect of FGF13-AS1 was also confirmed in T47D and MDA-MB-468 cells (Supplementary

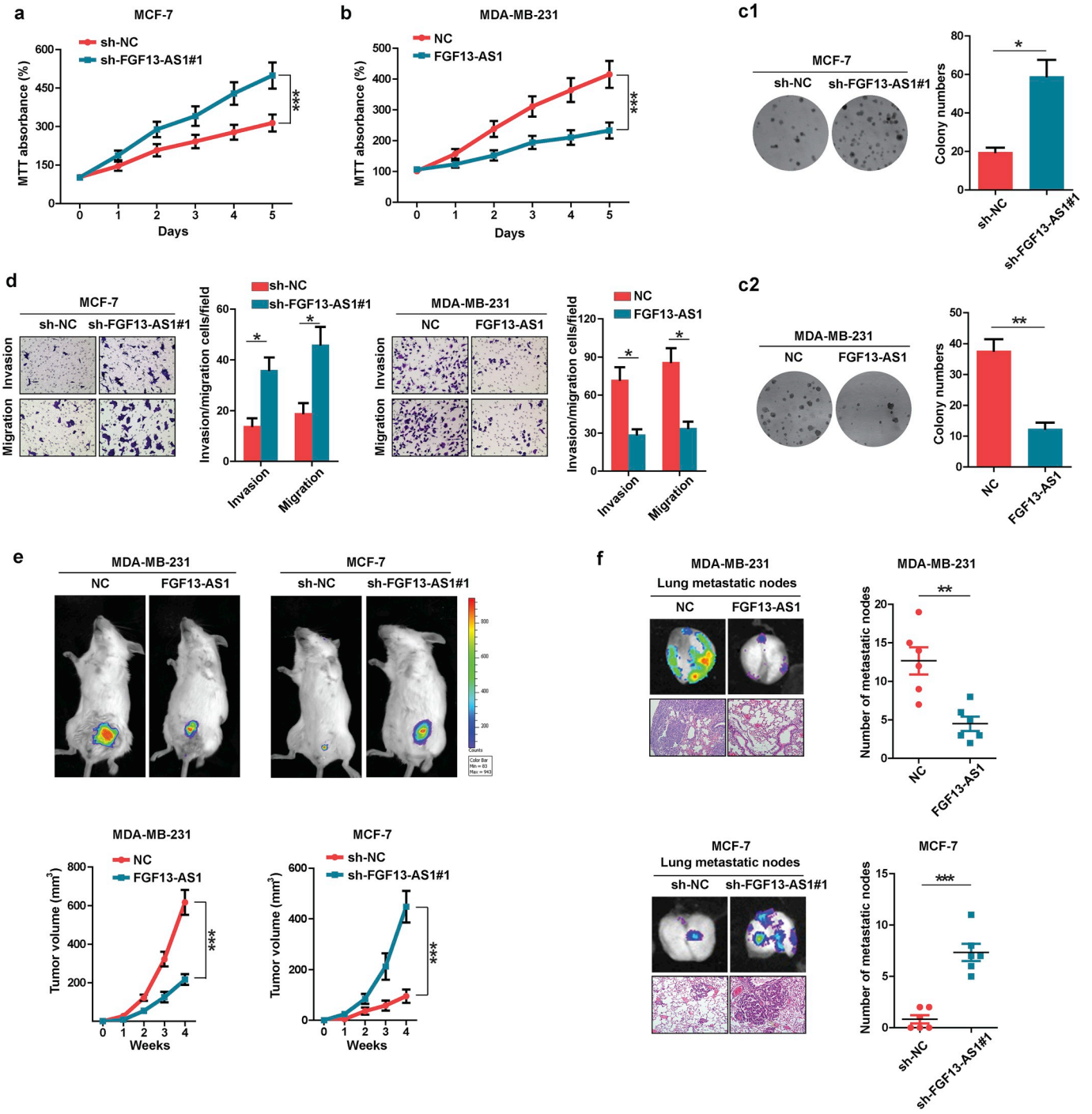

Fig. 2. FGF13-AS1 inhibits breast cancer cells proliferation, invasion and metastasis both in vitro and in vivo. (**a**) and (**b**) MTT assays were used to measure the effect of FGF13-AS1 overexpression or knockdown on proliferation of indicated cells. (**c**) Colony formation assays were performed to detect the effect of FGF13-AS1 overexpression or knockdown on proliferation of indicated cells. (**d**) Migration and invasion assays of indicated cells after FGF13-AS1 was overexpressed or knocked down. (**e**) and (**f**) Orthotopic breast tumor and lung metastatic mouse models were used to explore the tumorigenesis and metastasis of indicated cells after FGF13-AS1 overexpression or knockdown. *P < 0.05, **P < 0.01, ***P < 0.001.

Fig. 3a-d). Altogether, these data demonstrate that FGF13-AS1 inhibits breast cancer cells proliferation, invasion and metastasis both in vitro and in vivo.

3.3. FGF13-AS1 inhibits glycolysis and stemness features of BC cells

Given the crucial role of aerobic glycolysis in breast cancer proliferation and invasion [5], we next examined the effect of FGF13-AS1 on glucose metabolism of breast cancer cells. A glycolysis stress test was carried out to determine the glycolysis, glycolytic capacity and glycolytic reserve of indicated cells through measuring the extracellular acidification rate. As shown in Fig. 3a and Supplementary Fig. 2g, with the treatment of glucose, oligomycin or 2-DG, sh-FGF13-AS1 transfected MCF-7 cells exhibited markedly higher level of glycolysis, glycolytic capacity and glycolytic reserve compared with control cells. On the contrary, FGF13-AS1 overexpression was found to decrease the level of glycolysis, glycolytic capacity and glycolytic reserve in MDA-MB-231 cells. We also observed that depletion of FGF13-AS1 in MCF-

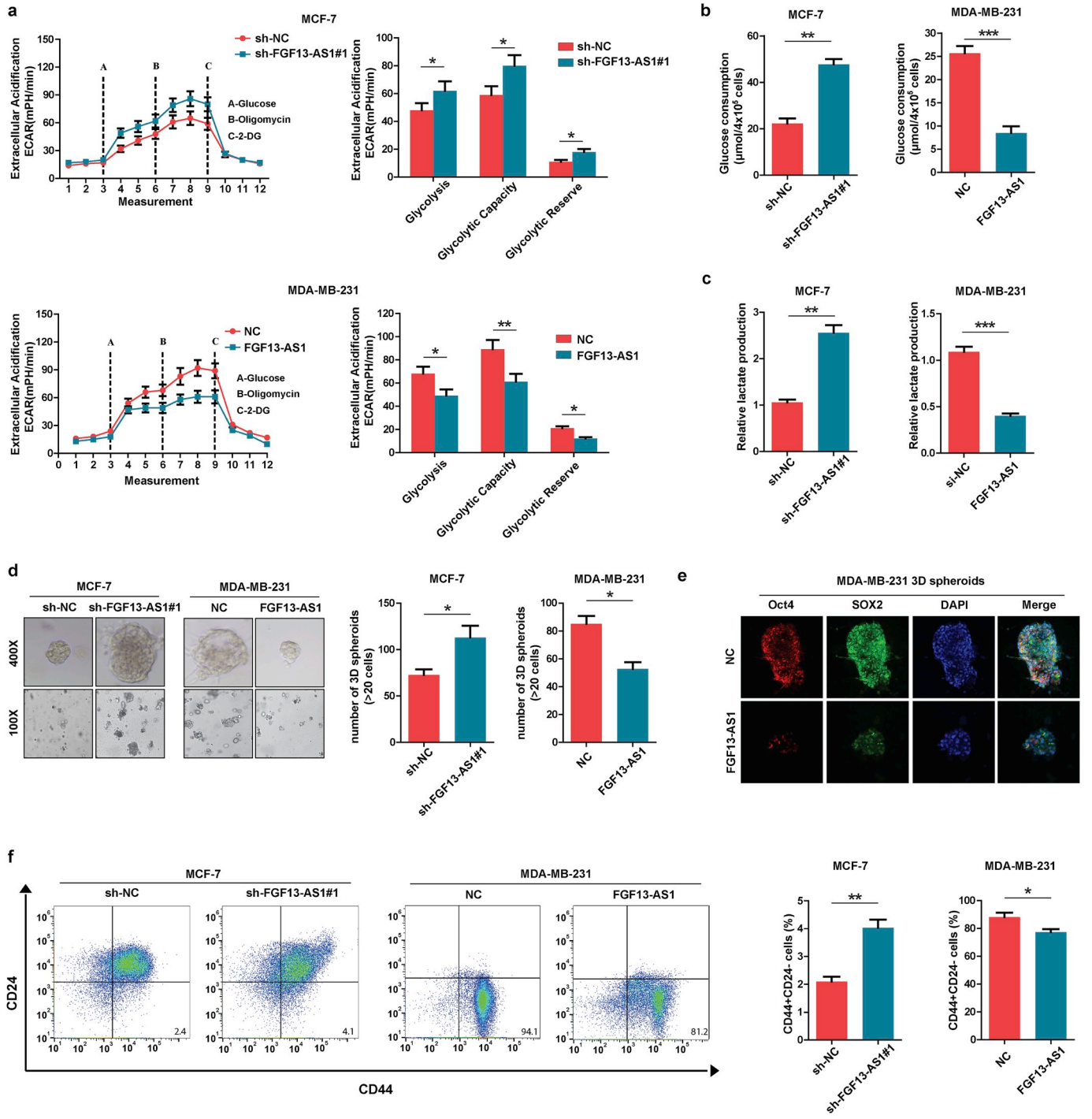

Fig. 3. FGF13-AS1 inhibits glycolysis and stemness feature of breast cancer cells. (**a**) After indicated treatment, ECAR was detected by the glycolysis stress test in breast cancer cells. The glycolysis, glycolytic capacity and glycolytic reserve of indicated cells were analyzed. (**b**) Glucose consumption was measured in breast cancer cells transfected with FGF13-AS1 or sh-FGF13-AS1. (**c**) Lactate production was tested in breast cancer cells transfected with FGF13-AS1 or sh-FGF13-AS1. (**d**) A 3D-cultured mammosphere model was used to measure the effect of FGF13-AS1 overexpression or knockdown on stemness of indicated cells. (**e**) IF staining of stemness markers (Sox2 and Oct4) in control or FGF13-AS1-transfected MDA-MB-231 cells. (**f**) Flow cytometry analysis was performed to evaluate the effects of FGF13-AS1 on cancer cells with the $CD44^{+}CD24^{-}$ phenotype. *P < 0.05, **P < 0.01, ***P < 0.001.

7 cells increased the glucose consumption and lactate production, whereas FGF13-AS1-transfected MDA-MB-231 cells consumed less glucose and released less lactate into the supernatant (Fig. 3b and c and Supplementary Fig. 2h and i). Collectively, these data suggest that FGF13-AS1 inhibits glycolysis of breast cancer cells. Another well-established reason for the unlimited proliferative potential of breast cancer cells is the existence of stem cells [24]. To test this, we generated a 3D-cultured mammosphere model to test the stem cell properties of the indicated cells. As expected, FGF13-AS1 transfection significantly limited the size and the number of spheroids derived from MDA-MB-231 cells. In contrast, knockdown of FGF13-AS1 increased the size and number of mammospheres derived from MCF-7 cells (Fig. 3d and Supplementary Fig. 2j). Furthermore, we performed immunofluorescence assays to evaluate the stemness markers of breast cancer cells. As indicated in Fig. 3e, the expression of OCT4 and SOX2 decreased in the mammospheres derived from FGF13-AS1-transfected

MDA-MB-231 cells. Flow cytometry analysis was also conducted to assess the effects of FGF13-AS1 on the $CD44^+CD24^-$ phenotype of breast cancer cells. The results showed that FGF13-AS1 overexpression decreased the percentage of $CD44^+CD24^-$ MDA-MB-231 cells, whereas sh-FGF13-AS1 transfection in MCF-7 cells increased the percentage of $CD44^+CD24^-$ cells (Fig. 3f and Supplementary Fig. 2k). To determine whether these data were reproducible in different breast cancer cell lines, we repeated the aforementioned assays in T47D and MDA-MB-468 cells. Consistently, the glycolysis and stemness properties were decreased in FGF13-AS1-overexpressed MDA-MB-468 cells but increased in FGF13-AS1-knockdown T47D cells (Supplementary Fig. 4). To conclude, FGF13-AS1 restrains the stemness feature of breast cancer cells.

3.4. FGF13-AS1 suppresses the expression of Myc by decreasing Myc mRNA stability

It is well known that HIF-1α and Myc are important oncogenic transcription factors that play central regulatory roles in cancer cell glycolysis [25]. We therefore set out to detect whether FGF13-AS1 inhibited glycolysis by affecting these two factors. As indicated in Fig. 4a, FGF13-AS1 overexpression significantly decreased the expression of Myc, but not HIF-1α. Coincidentally, Myc was also reported to be associated with stem cell properties in breast cancer [12]. Thus, we proposed that FGF13-AS1 inhibited glycolysis and stemness feature of breast cancer cells by affecting Myc expression. We next detected the mRNA level of Myc in FGF13-AS1-transfected cells; decreased mRNA levels of Myc were also confirmed by qRT-PCR analysis (Fig. 4b). Since the subcellular location of Lnc RNAs generally determines the function, we performed fluorescence in situ hybridization (FISH) of FGF13-AS1 followed by immunofluorescent staining of Myc to investigate the mechanism by which FGF13-AS1 downregulated Myc expression. The results revealed that FGF13-AS1 localized mainly in the cytoplasm of breast cancer cells, which indicated the potential for post-transcriptional regulation of Myc by FGF13-AS1. Additionally, overexpression of FGF13-AS1 markedly decreased the expression of Myc in MDA-MB-231 cells, whereas FGF13-AS1 knockdown enhanced the Myc expression in MCF-7 cells. These results double confirmed the inhibitory effect of FGF13-AS1 on Myc (Fig. 4c). Again, we performed qRT-PCR analysis to detect the expression of FGF13-AS1 by RNA fractionation of the nucleus and cytoplasm, indicating that it resided in cytoplasm (Fig. 4d). Based on luciferase reporter assays, we found that FGF13-AS1 did not transcriptionally regulate Myc (Fig. 4e). Therefore, we next explored whether FGF13-AS1 regulated the synthesis or degradation of Myc mRNA. As expected, with the treatment of actinomycin D, an inhibitor of RNA synthesis, FGF13-AS1-transfected MDA-MB-231 cells showed a dramatically shorter half-life of Myc mRNA while knockdown of FGF13-AS1 in MCF-7 cells markedly increased the half-life of Myc mRNA (Fig. 4f and Supplementary Fig. 5a). To confirm that FGF13-AS1 suppresses glycolysis and stemness properties in breast cancer cells by down-regulating Myc, we compared the effects of FGF13-AS1, Myc and 10058-F4 (an inhibitor of Myc) on MDA-MB-231 cells. As shown in Fig. 4g and h, Myc overexpression restored the decreased lactate production and glucose consumption of FGF13-AS1-transfected cells, whereas 10058-F4 inhibited lactate secretion and glucose consumption to a comparable degree as FGF13-AS1 in MDA-MB-231 cells. Similar effects were also found on cell proliferation (Fig. 4i). Moreover, FGF13-AS1 markedly decreased the size and number of 3D-cultured spheroids of MDA-MB-231 cells, while Myc transfection rescued the phenotype of FGF13-AS1 in MDA-MB-231 cells (Fig. 4j). We also compared the effects of sh-FGF13-AS1, si-Myc and Myc on MCF-7 cells, which confirmed that knockdown of FGF13-AS1 promoted glycolysis and stemness properties in breast cancer cells by up-regulating Myc (Supplementary Fig. 5b-e). In conclusion, FGF13-AS1 suppresses breast cancer glycolysis and stemness properties by decreasing the stability of Myc mRNA.

3.5. FGF13-AS1 directly interacts with IGF2BPs and reduces the association between Myc mRNA and IGF2BPs

Previous studies have reported that all three IGF2BP proteins (IGF2BP1, IGF2BP2, IGF2BP3) physically prevents Myc mRNA degradation by binding to the consensus sequence containing the 'GGAC' m^6A core motif [26]. Interestingly, we found that FGF13-AS1 contained a potential binding site for IGF2BP proteins that was similar to the m^6A core motif (Fig. 5a). Meanwhile, aforementioned data showed that FGF13-AS1 mainly localized in the cytoplasm where the regulation of Myc mRNA stability is permitted. Therefore, we speculated that FGF13-AS1 might bind IGF2BPs and disrupt the interaction between IGF2BPs and Myc mRNA. To test this idea, we performed RNA immunoprecipitation (RIP) assays using IGF2BP1 antibody in MDA-MB-231 and MCF-7 cells. We observed a marked enrichment of FGF13-AS1 pulled down by IGF2BP1 antibody compared with the IgG control antibody (Fig. 5b). Of note, Myc mRNA was also observed, which was consistent with previous studies. We next performed RNA pull-down assays to further confirm the interaction between IGF2BP1 and FGF13-AS1. As indicated in Fig. 5c, an enhancement of IGF2BP1 was found in the presence of FGF13-AS1, but not the antisense RNA. These results indicate a specific interaction between FGF13-AS1 and IGF2BP proteins.

To further explore whether FGF13-AS1 disturbs the association between IGF2BP proteins and Myc mRNA by interacting with IGF2BP proteins, RIP assays were carried out using IGF2BP1 antibody in breast cancer cells. Based on the basal expression level of FGF13-AS1 in breast cancer cells (Fig. 1e), we overexpressed FGF13-AS1 in MDA-MB-231 cells and knockdown FGF13-AS1 in MCF-7 cells to see the variation of Myc that bound to IFG2BP1. We observed that FGF13-AS1 transfection significantly decreased the level of Myc mRNA that was associated with IGF2BP1 protein, whereas knockdown of FGF13-AS1 increased the IGF2BP1-binding Myc mRNA level (Fig. 5d and e). To investigate whether FGF13-AS1 inhibits the stability of Myc mRNA directly through binding IGF2BP proteins, we examined the mRNA and protein level of Myc in IGF2BPs-knockdown cells. We first confirmed the IGF2BPs knockdown efficiency by detecting the expression level of Myc, a downstream target of IGF2BP proteins [26] (Supplementary Fig. 6a). Results showed that FGF13-AS1 transfection was unable to regulate the level of Myc mRNA and protein in IGF2BPs-knockdown cells (Fig. 5f and g and Supplementary Fig. 6b and c); the half-life of Myc mRNA was unaffected as well (Fig. 5h and Supplementary Fig. 6d). Functionally, FGF13-AS1 did not change the lactate secretion, proliferation or invasion of si-IGF2BPs-transfected MDA-MB-231 cells (Fig. 5i–k and Supplementary Fig. 6e, g). These results reveal that FGF13-AS1 functions by binding IGF2BPs and subsequently reducing the stabilization of Myc mRNA by IGF2BP proteins.

3.6. Myc transcriptionally inhibits FGF13-AS1

Since we found that FGF13-AS1 was downregulated in breast cancer, we further explored the transcriptional regulation of FGF13-AS1. As a transcription factor, Myc was reported to function as a negative regulator in LncRNA biogenesis [27]. Thus, we next examined the possibility that Myc transcriptionally regulated FGF13-AS1 using bioinformatics software. The LASAGNA-Search 2.0 software predicted a potential binding site for Myc in the promoter region of FGF13-AS1 (Fig. 6a). Reporter plasmids containing the putative binding sequence within the FGF13-AS1 promoter were made to measure the effect of Myc on FGF13-AS1 transcription. As shown in Fig. 6b, co-transfection of Myc and FGF13-AS1-reporter plasmid in 293T cells led to a reduction of luciferase activity, which decreased in response to the dose of Myc. However, plasmids containing mutation of the Myc binding site in FGF13-AS1 promoter region failed to show the decreased luciferase activity and abrogated the response to the dose of Myc (Fig. 6b). Moreover, chromatin immunoprecipitation (ChIP) assays confirmed

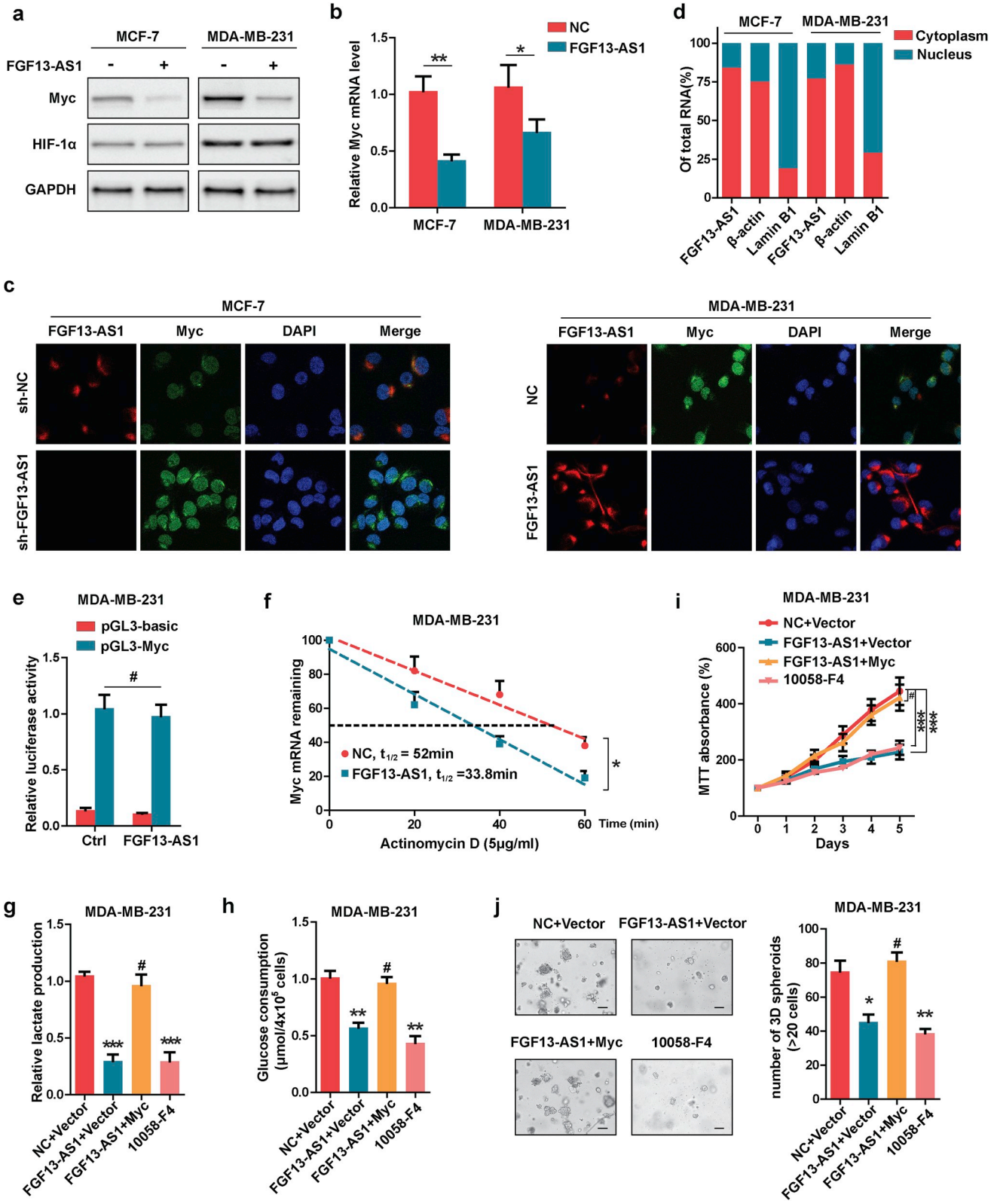

Fig. 4. FGF13-AS1 suppresses the expression of Myc by decreasing Myc mRNA stability. (**a**) Western blot assays were used to detect the Myc protein levels in FGF13-AS1-transfected or control breast cancer cells. After serum starvation for 24 h, the HIF-1α protein levels of indicated cells were also measured. β-actin was used as an internal control. (**b**) qRT-PCR was used to detect the mRNA level of Myc in FGF13-AS1-transfected breast cancer cells. (**c**) Combined FISH/IF assays showed FGF13-AS1 located mainly in the cytoplasm of breast cancer cells and the FGF13-AS1 expression negatively correlated with the expression of Myc. (**d**) qRT-PCR was used to measure the nuclear and cytoplasmic FGF13-AS1. (**e**) Luciferase reporter assays showed that FGF13-AS1 failed to influence Myc promoter transcriptional activity in MDA-MB-231 cells. (**f**) Myc mRNA levels were measured using actinomycin D mRNA stability assays in MDA-MB-231 cells. Myc mRNA was normalized to 18 S RNA, and the half-life of Myc mRNA was calculated in FGF13-AS1-transfected or control cells. (**g**) and (**h**) Myc overexpression restored the decreased lactate production and glucose consumption of FGF13-AS1-transfected cells. 10058-F4 inhibited the lactate secretion and glucose consumption to a comparable degree to FGF13-AS1 in MDA-MB-231 cells. (**i**) The proliferative ability of indicated cells was measured using MTT assays. (**j**) The size and number of 3D-cultured spheroids of indicated cells were measured by 3D culture system. *P < 0.05, **P < 0.01, ***P < 0.001, # represents no statistical significance.

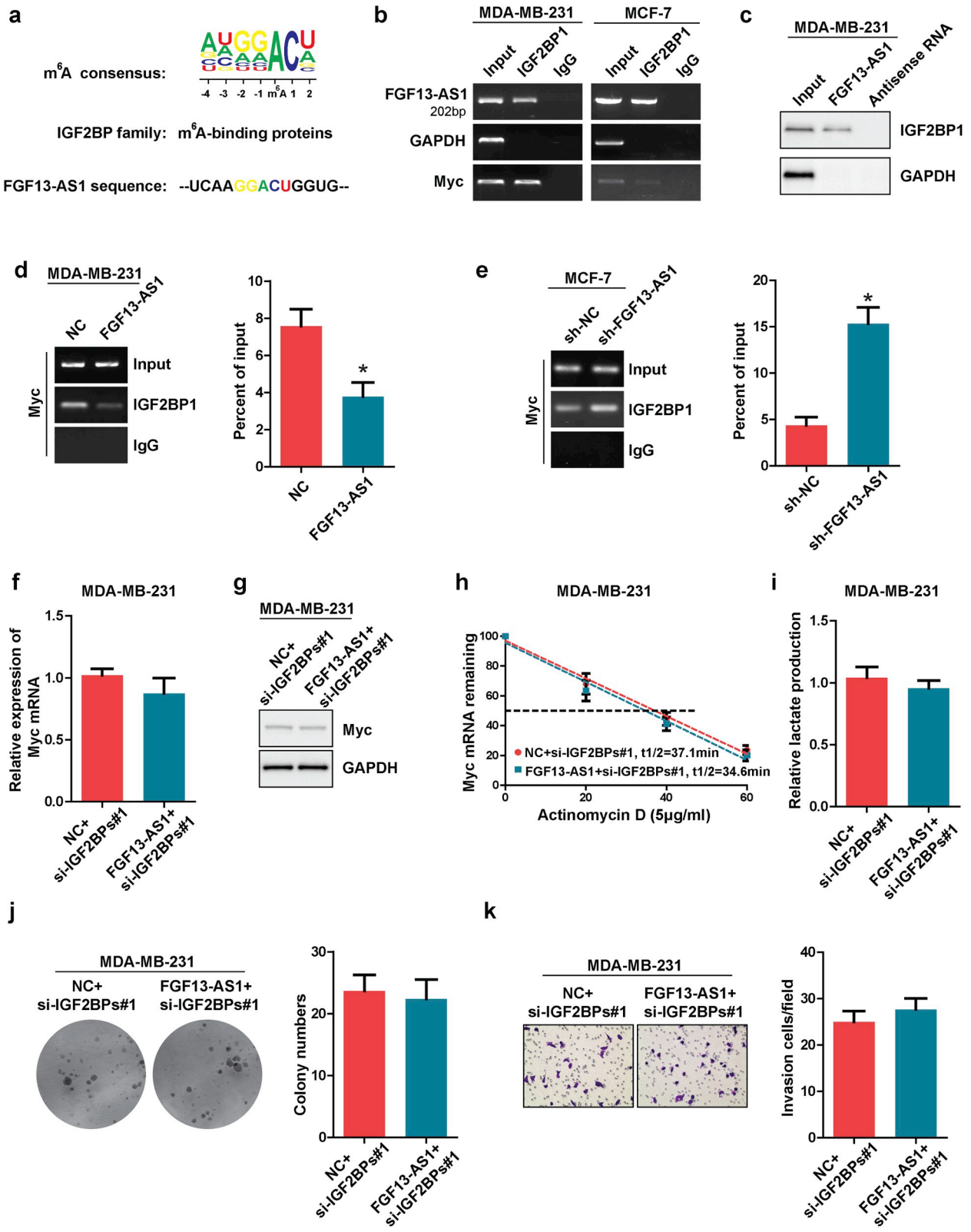

Fig. 5. FGF13-AS1 directly interacts with IGF2BPs and reduces the stabilization of Myc mRNA by IGF2BPs. (**a**) Potential binding site of IGF2BPs in FGF13-AS1 sequence. (**b**) RIP assays were performed using IGF2BP1 antibody or IgG, and specific primers were used to detect FGF13-AS1, GAPDH and Myc in MDA-MB-231 and MCF-7 cells. (**c**) RNA pull-down assays were performed using FGF13-AS1 and antisense RNA. GAPDH was used as the control. (**d**) and (**e**) After transfection of FGF13-AS1 or sh-FGF13-AS1 in breast cancer cells, RIP assays were performed using anti-FGF13-AS1 and non-specific IgG. The levels of RIP-derived Myc mRNA were determined by qRT-PCR and expressed as a percentage of the input. (**f**) and (**g**) IGF2BPs-knockdown cells were transfected with FGF13-AS1 or control RNA, the mRNA and protein level of Myc were measured by qRT-PCR and western blot assays. (**h**) The half-life of Myc mRNA was measured in indicated cells. (**i**) FGF13-AS1 transfection failed to reduce the lactate production of IGF2BP1-knockdown cells. (**j**) and (**k**) Colony formation and transwell assays were performed to detect the proliferative and invasive ability of indicated cells. *P < 0.05.

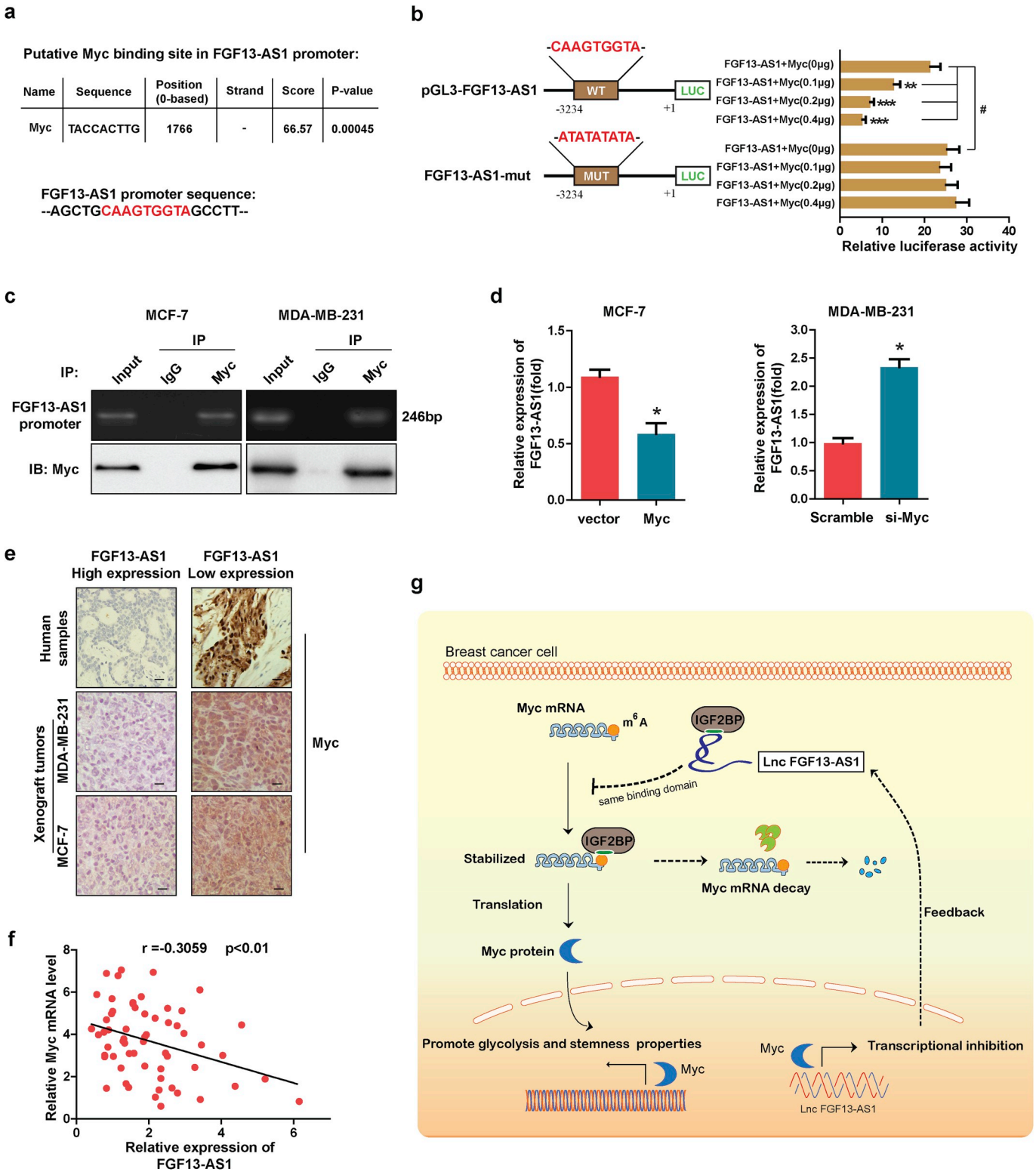

Fig. 6. Myc transcriptionally inhibits FGF13-AS1. (**a**) The putative Myc binding site in the FGF13-AS1 promoter as predicted by bioinformatics software. (**b**) Wild-type or mutant FGF13-AS1 promoter reporter constructs and various amounts of Myc overexpression plasmids were co-transfected into 293T cells. (**c**) ChIP assays were performed in breast cancer cells using Myc antibodies or IgG. The FGF13-AS1 promoter fragment was detected by specific primers. (**d**) qRT-PCR was used to detect the expression of FGF13-AS1 in indicated breast cancer cells. (**e**) Representative IHC staining images of Myc expression in high/low FGF13-AS1 expressing breast cancer tissues or xenograft tumor tissues. (**f**) The correlation between Myc and FGF13-AS1 expression in breast cancer patients. (**g**) Schematic diagram of the mechanism that FGF13-AS1 regulates the FGF13-AS1/IGF2BPs/Myc feedback loop. *P < 0.05, **P < 0.01, ***P < 0.001, # represents no statistical significance.

that this putative binding site in the FGF13-AS1 promoter effectively bound to Myc protein in breast cancer cells (Fig. 6c). Because the basal level of Myc was low in MCF-7 cells and high in MDA-MB-231 cells (Fig. 4a), so we overexpressed Myc in MCF-7 cells for the gain of function assays and knockdown Myc in MDA-MB-231 cells for the loss of function assays. The results showed that Myc transfection in MCF-

7 cells indeed downregulated the expression of FGF13-AS1, while knockdown of Myc increased the FGF13-AS1 expression in MDA-MB-231 cells (Fig. 6d). To explore the expression patterns of FGF13-AS1 and Myc in clinical samples, immunohistochemistry (IHC) staining and qRT-PCR were performed. We revealed that cancer tissues with high expression of FGF13-AS1 tended to express low levels of Myc protein both in clinical samples and xenograft tumors, and vice versa (Fig. 6e). An inverse expression pattern between FGF13-AS1 and Myc mRNA was also detected in a group of 60 patients (Fig. 6f). Taken together, these data support that Myc inhibits the transcription of FGF13-AS1, thus exerting an autoregulatory feedback loop.

4. Discussion

In this study, we showed that FGF13-AS1 was downregulated in breast cancer tissues and highly metastatic breast cancer cell lines. Meanwhile, FGF13-AS1 expression was negatively correlated with prognosis of patients. As a tumor suppressor, FGF13-AS1 inhibited breast cancer cell proliferation, migration and invasion by impairing glycolysis and stemness properties. To explore the downstream targets that might explain the role of FGF13-AS1 in breast cancer, we identified that Myc mRNA half-life was reduced by FGF13-AS1 overexpression based on the following results: (1) the mRNA and protein level of Myc were decreased by FGF13-AS1 transfection in breast cancer cells; (2) immunofluorescence staining indicated that FGF13-AS1 was expressed mainly in the cytoplasm. (3) luciferase reporter assays showed that Myc was not transcriptionally regulated. Additionally, we found that FGF13-AS1 reduced the half-life of Myc mRNA by binding IGF2BPs and disrupting the interaction between IGF2BPs and Myc mRNA, which was supported by RIP assays. Furthermore, we reported that FGF13-AS1 was under the control of Myc protein. These data present a tumor suppressive network by a FGF13-AS1/IGF2BPs/Myc feedback loop.

FGF13-AS1 was identified as one of the 25 downregulated lncRNAs in breast cancer through analyzing data from two cohorts and TCGA by another group of our lab [23]. However, no experiments had been performed to confirm the expression of FGF13-AS1 in breast cancer. Therefore, we detected the expression of FGF13-AS1 in breast cancer tissues and cell lines for the first time. Consistent with the sequencing data from datasets, we found that FGF13-AS1 expression was decreased in breast cancer tissues and high-metastatic cell lines. Functional assays such as MTT, colony formation, transwell, and an in vivo xenograft mouse model were used to evaluate the effect of FGF13-AS1 on breast cancer cells. These data certified that FGF13-AS1 functioned as a tumor suppressor in breast cancer by repressing glycolysis and stem-like properties. In accordance with our data, previous studies also reported that lncRNAs played important roles in tumor glycolytic metabolism and stemness maintenance [28,29]. For example, lncRNA PCGEM1 could influence a variety of glycolytic metabolism related pathways to regulate cancer glycolysis; LncRNA NEAT1 was also proven to promote stemness in lung cancer [30,31]. Based on these findings, we confirmed that FGF13-AS1 could be recognized as a tumor suppressive lncRNA in breast cancer.

The expression of Myc is deregulated in various types of cancers. In breast cancer, Myc is upregulated in 30%–50% of high-grade tumors [32]. Myc functions as an oncogenic transcription factor and plays vital roles in multiple processes of cancer progression, including glycolysis and stemness properties. Our data demonstrated that FGF13-AS1 could specifically bind IGF2BPs, as it carried a potential IGF2BPs binding motif which was also essential for the interaction between IGF2BPs and Myc mRNA. Thus, FGF13-AS1 could disrupt the interaction between IGF2BPs and Myc mRNA, and subsequently lead to the instability and decay of Myc mRNA. A similar regulatory mechanism was also found in another article. LncRNA ROR was reported to carry the potential hnRNP I binding motifs which was sufficient for the repression of p53 mRNA [19]. Conversely, another study showed that lncRNA GHET1 promoted gastric cancer progression by binding IGF2BP1 and subsequently enhanced the interaction between IGF2BP1 and Myc RNA, which presented quite the opposite effect of FGF13-AS1 [33]. However, they did not explore the binding site of IGF2BP1 within the GHET1 sequence. Therefore, our data showed a more detailed elaboration of the mechanism that FGF13-AS1 regulated the stability of Myc mRNA. Of note, lncRNAs can regulate downstream targets in many complicated ways. For instance, lncRNAs may regulate gene expression by binding to the promoter region and changing the histone markers and chromatin state [15]; they may also interact with RNA-binding proteins and alter the activity or expression of the proteins, which may be involved in cancer biology [16,34]. Thus, there might be other signaling pathways mediating the function of FGF13-AS1 in breast cancer, which remain to be explored.

Another interesting finding in our study was the transcriptional regulation of FGF13-AS1 by Myc. By using luciferase reporter assays, ChIP assays and the analysis of clinical samples, we showed that Myc could bind to the promoter of FGF13-AS1 and downregulate it expression. Consistently, previous studies have shown that, on one hand, Myc can transcriptionally activate multiple lncRNAs, such as PVT1, CCAT1 and H19 [35–37]. On the other hand, some lncRNAs that have tumor suppressor roles in cancer, can be transcriptionally repressed by Myc [38]. Thus, to some extent, this autoregulatory feedback loop might elucidate the importance of the FGF13-AS1-Myc interplay network and verify the crucial roles of FGF13-AS1 and Myc in breast cancer.

Authors' contribution

FM and XL carried out most of the experimental work; SZ conducted the analysis of data; WL and CL performed the molecular cloning and animal experiments; FM and CQ designed the project and wrote the manuscript. All authors have read and approved the manuscript.

Ethics approval and consent to participate

This study was approved by the Ethical Committee of Harbin Medical University. The study was performed according to the ethical standards of Declaration of Helsinki and patient consent for the use of tissues was obtained prior to the initiation of the study. Additionally, the animal experiments were performed in accordance with the Guide for the Administration of Affairs Concerning Experimental Animals.

Declaration of interest

None.

Conflicts of interest statement

The authors declare no conflict of interests.

Availability of data and materials

All data generated or analyzed during this study are included in this published article.

Consent for publication

We have obtained consents to publish this paper from all the participants of this study.

Funding

This work was supported by the National Natural Science Foundation of China (81372837, H1622).

Acknowledgements

We thank Department of General Surgery, the Second Affiliated Hospital of Harbin Medical University 246 Xuefu Street, Nangang

District, Harbin, China for providing the breast cancer samples and related clinical data. We thank Michelle Chadwick who is a cancer researcher in Rutgers, Cancer Institute of New Jersey for helping us revise the manuscript.

Abbreviations

Lnc FGF13-AS1	long non-coding RNA FGF13-AS1
TCGA	the cancer genome atlas
IGF2BPs	insulin-like growth factor 2 mRNA binding proteins
LDHA	lactate dehydrogenase
FISH	Fluorescence in situ hybridization
ECAR	extracellular acidification rate
ChIP	chromatin-immunoprecipitation
RIP	RNA immunoprecipitation
FISH	fluorescence in situ hybridization
IHC	immunohistochemistry

Appendix A. Supplementary data

Supplementary data to this article can be found online at https://doi.org/10.1016/j.canlet.2019.02.008.

References

[1] A. Jemal, F. Bray, M.M. Center, J. Ferlay, E. Ward, D. Forman, Global cancer statistics, CA A Cancer J. Clin. 61 (2011) 69–90.
[2] F. Ma, J. Zhang, L. Zhong, L. Wang, Y. Liu, Y. Wang, L. Peng, B. Guo, Upregulated microRNA-301a in breast cancer promotes tumor metastasis by targeting PTEN and activating Wnt/β-catenin signaling, Gene 535 (2014) 191–197.
[3] W. Hong, E. Dong, The past, present and future of breast cancer research in China, Cancer Lett. 351 (2014) 1–5.
[4] A. Filipova, M. Seifrtova, J. Mokry, J. Dvorak, M. Rezacova, S. Filip, D. Diaz-Garcia, Breast cancer and cancer stem cells: a mini-review, Tumori 100 (2014) 363–369.
[5] F. Ma, L. Zhang, L. Ma, Y. Zhang, J. Zhang, B. Guo, MiR-361-5p inhibits glycolytic metabolism, proliferation and invasion of breast cancer by targeting FGFR1 and MMP-1, J. Exp. Clin. Canc. Res. 36 (2017) 158.
[6] C.V. Dang, MYC, metabolism, cell growth, and tumorigenesis, Cold Spring Harbor Perspect. Med. 3 (2013) a014217.
[7] J.S. Parker, M. Mullins, M.C. Cheang, S. Leung, D. Voduc, T. Vickery, S. Davies, C. Fauron, X. He, Z. Hu, Supervised risk predictor of breast cancer based on intrinsic subtypes, J. Clin. Oncol. 27 (2009) 1160.
[8] S. Loi, B. Haibe-Kains, S. Majjaj, F. Lallemand, V. Durbecq, D. Larsimont, A.M. Gonzalez-Angulo, L. Pusztai, W.F. Symmans, A. Bardelli, PIK3CA mutations associated with gene signature of low mTORC1 signaling and better outcomes in estrogen receptor–positive breast cancer, Proc. Natl. Acad. Sci. Unit. States Am. 107 (2010) 10208–10213.
[9] S.B. McMahon, MYC and the control of apoptosis, Cold Spring Harbor Perspect. Med. 4 (2014) a014407.
[10] J.-w. Kim, P. Gao, Y.-C. Liu, G.L. Semenza, C.V. Dang, Hypoxia-inducible factor 1 and dysregulated c-Myc cooperatively induce vascular endothelial growth factor and metabolic switches hexokinase 2 and pyruvate dehydrogenase kinase 1, Mol. Cell Biol. 27 (2007) 7381–7393.
[11] C.V. Dang, J.-w. Kim, P. Gao, J. Yustein, The interplay between MYC and HIF in cancer, Nat. Rev. Canc. 8 (2008) 51.
[12] L. Xu, S. Li, W. Zhou, Z. Kang, Q. Zhang, M. Kamran, J. Xu, D. Liang, C. Wang, Z. Hou, p62/SQSTM1 enhances breast cancer stem-like properties by stabilizing MYC mRNA, Oncogene 36 (2017) 304.
[13] E.P. Consortium, Identification and analysis of functional elements in 1% of the human genome by the ENCODE pilot project, Nature 447 (2007) 799.
[14] J.E. Wilusz, H. Sunwoo, D.L. Spector, Long noncoding RNAs: functional surprises from the RNA world, Genes Dev. 23 (2009) 1494–1504.
[15] R.A. Gupta, N. Shah, K.C. Wang, J. Kim, H.M. Horlings, D.J. Wong, M.-C. Tsai, T. Hung, P. Argani, J.L. Rinn, Long non-coding RNA HOTAIR reprograms chromatin state to promote cancer metastasis, Nature 464 (2010) 1071.
[16] M. Guttman, J. Donaghey, B.W. Carey, M. Garber, J.K. Grenier, G. Munson, G. Young, A.B. Lucas, R. Ach, L. Bruhn, lincRNAs act in the circuitry controlling pluripotency and differentiation, Nature 477 (2011) 295.
[17] Y. Zhao, Y. Liu, L. Lin, Q. Huang, W. He, S. Zhang, S. Dong, Z. Wen, J. Rao, W. Liao, The lncRNA MACC1-AS1 promotes gastric cancer cell metabolic plasticity via AMPK/Lin28 mediated mRNA stability of MACC1, Mol. Canc. 17 (2018) 69.
[18] J.L. Rinn, H.Y. Chang, Genome regulation by long noncoding RNAs, Annu. Rev. Biochem. 81 (2012) 145–166.
[19] A. Zhang, N. Zhou, J. Huang, Q. Liu, K. Fukuda, D. Ma, Z. Lu, C. Bai, K. Watabe, Y.-Y. Mo, The human long non-coding RNA-RoR is a p53 repressor in response to DNA damage, Cell Res. 23 (2013) 340.
[20] P.J. Batista, H.Y. Chang, Cytotopic localization by long noncoding RNAs, Curr. Opin. Cell Biol. 25 (2013) 195–199.
[21] X. Han, F. Yang, H. Cao, Z. Liang, Malat1 regulates serum response factor through miR-133 as a competing endogenous RNA in myogenesis, FASEB J 29 (2015) 3054–3064.
[22] C. Wahlestedt, Targeting long non-coding RNA to therapeutically upregulate gene expression, Nat. Rev. Drug Discov. 12 (2013) 433–446.
[23] S. Xu, D. Kong, Q. Chen, Y. Ping, D. Pang, Oncogenic long noncoding RNA landscape in breast cancer, Mol. Canc. 16 (2017) 129.
[24] N. Yan, L. Xu, X. Wu, L. Zhang, X. Fei, Y. Cao, F. Zhang, GSKJ4, an H3K27me3 demethylase inhibitor, effectively suppresses the breast cancer stem cells, Exp. Cell Res. 359 (2017) 405–414.
[25] X. Guo, Y. Zhu, X. Hong, M. Zhang, X. Qiu, Z. Wang, Z. Qi, X. Hong, miR-181d and c-myc-mediated inhibition of CRY2 and FBXL3 reprograms metabolism in colorectal cancer, Cell Death Dis. 8 (2017) e2958.
[26] H. Huang, H. Weng, W. Sun, X. Qin, H. Shi, H. Wu, B.S. Zhao, A. Mesquita, C. Liu, C.L. Yuan, Recognition of RNA N 6-methyladenosine by IGF2BP proteins enhances mRNA stability and translation, Nat. Cell Biol. 20 (2018) 285.
[27] M.J. Hamilton, M.D. Young, S. Sauer, E. Martinez, The interplay of long non-coding RNAs and MYC in cancer, AIMS biophysics 2 (2015) 794.
[28] C. Fan, Y. Tang, J. Wang, F. Xiong, C. Guo, Y. Wang, S. Zhang, Z. Gong, F. Wei, L. Yang, Role of long non-coding RNAs in glucose metabolism in cancer, Mol. Canc. 16 (2017) 130.
[29] J. Deng, M. Yang, R. Jiang, N. An, X. Wang, B. Liu, Long non-coding RNA HOTAIR regulates the proliferation, self-renewal capacity, tumor formation and migration of the cancer stem-like cell (CSC) subpopulation enriched from breast cancer cells, PLoS One 12 (2017) e0170860.
[30] C.-L. Hung, L.-Y. Wang, Y.-L. Yu, H.-W. Chen, S. Srivastava, G. Petrovics, H.-J. Kung, A long noncoding RNA connects c-Myc to tumor metabolism, Proc. Natl. Acad. Sci. Unit. States Am. 111 (2014) 18697–18702.
[31] P. Jiang, A. Chen, X. Wu, M. Zhou, I. ul Haq, Z. Mariyam, Q. Feng, NEAT1 acts as an inducer of cancer stem cell-like phenotypes in NSCLC by inhibiting EGCG-upregulated CTR1, J. Cell. Physiol. 233 (2018) 4852–4863.
[32] J. Blancato, B. Singh, A. Liu, D. Liao, R. Dickson, Correlation of amplification and overexpression of the c-myc oncogene in high-grade breast cancer: FISH, in situ hybridisation and immunohistochemical analyses, Br. J. Canc. 90 (2004) 1612.
[33] F. Yang, X. Xue, L. Zheng, J. Bi, Y. Zhou, K. Zhi, Y. Gu, G. Fang, Long non-coding RNA GHET1 promotes gastric carcinoma cell proliferation by increasing c-Myc mRNA stability, FEBS J 281 (2014) 802–813.
[34] Q. Gou, L. Gao, X. Nie, W. Pu, J. Zhu, Y. Wang, X. Liu, S. Tan, J.-K. Zhou, Y. Gong, Long noncoding RNA AB074169 inhibits cell proliferation via modulation of KHSRP-mediated p21 expression in papillary thyroid carcinoma, Cancer Res. 78 (2018) 4163–4174 canres. 3766.2017.
[35] L. Carramusa, F. Contino, A. Ferro, L. Minafra, G. Perconti, A. Giallongo, S. Feo, The PVT-1 oncogene is a Myc protein target that is overexpressed in transformed cells, J. Cell. Physiol. 213 (2007) 511–518.
[36] X. He, X. Tan, X. Wang, H. Jin, L. Liu, L. Ma, H. Yu, Z. Fan, C-Myc-activated long noncoding RNA CCAT1 promotes colon cancer cell proliferation and invasion, Tumor Biol. 35 (2014) 12181–12188.
[37] D. Barsyte-Lovejoy, S.K. Lau, P.C. Boutros, F. Khosravi, I. Jurisica, I.L. Andrulis, M.S. Tsao, L.Z. Penn, The c-Myc oncogene directly induces the H19 noncoding RNA by allele-specific binding to potentiate tumorigenesis, Cancer Res. 66 (2006) 5330–5337.
[38] T. Kim, R. Cui, Y.-J. Jeon, P. Fadda, H. Alder, C.M. Croce, MYC-repressed long noncoding RNAs antagonize MYC-induced cell proliferation and cell cycle progression, Oncotarget 6 (2015) 18780.